A quasi-realtime x-ray microtomography system at the Advanced Photon Source

Yuxin Wang[a], Francesco De Carlo[a], Ian Foster[b], Joseph Insley[b],
Carl Kesselman[c], Peter Lane[b], Gregor von Laszewski[b],
Derrick Mancini[a], Ian McNulty[a], Mei-Hui Su[c], Brian Tieman[a]

[a]Advanced Photon Source, Argonne National Laboratory
[b]Mathematics and Computer Science Division, Argonne National Laboratory
[c]Information Sciences Institute, University of Southern California

ABSTRACT

The combination of high-brilliance x-ray sources, fast detector systems, wide-bandwidth networks, and parallel computers can substantially reduce the time required to acquire, reconstruct, and visualize high-resolution three-dimensional tomographic data sets. A quasi-realtime computed x-ray microtomography system has been implemented at the 2BM beamline at the Advanced Photon Source in Argonne National Laboratory. With this system, a complete tomographic data set can be collected in about 15 minutes at the beamline, and immediately after each projection is obtained, it is transferred to the Mathematics and Computing Sciences Division where preprocessing and reconstruction calculations are performed concurrently with the data acquisition by a SGI parallel computer. The reconstruction results, once completed, are rapidly transferred to a visualization computer, which performs the volume rendering calculations. Rendered images of the reconstructed data are available for viewing back at the beamline experiment station minutes after the data acquisition was complete. The fully pipelined data acquisition and reconstruction system also gives us the option to acquire the tomographic data set in several cycles, initially with coarse then with fine angular steps. At present the projections are acquired with a straight-ray projection imaging scheme using 5-20 KeV hard x rays in either phase or amplitude contrast mode at a few μm resolution. In the future, we expect to increase the resolution of the projections to below 100 nm by using a focused x-ray beam at the 2-ID-B beamline and to reduce the combined acquisition and computation time to one-minutes scale with improvments in the detectors, network links, and computation algorithms.

Keywords: realtime, x-ray microtomography, supercomputing, globus, hdf, nexus

1. INTRODUCTION

By provding high-brilliance x rays for crystallography, spectroscopy and microimaging, synchrotron radiation facilities are playing an increasingly important role in reseach in biology, physics, material, and environmental sciences. Many applications use tomographic imaging technique to produce a three dimensional representation of a sample. Using 5-20 KeV hard x rays, it is possible to image samples of a few mm thickness at 1 μm resolution in three-dimensions[1–3] while using soft x rays with a few hundred eV to 2 KeV energy, small samples of a few μm thickness can be imaged at 50 - 100 nm resolution.[4–6] In principle, the brilliance of third generation synchrotron radiation facilities allows high resolution images to be acquired at the rate of tens of images per second if photon statistics were the only concern. This suggests that if a high speed data acquistion is implemented to take advantage of the high photon flux, it is possible to acquire enough images for a tomographic data set in a few seconds to a few minutes so that time resolved observations in seconds to minutes scale can be made at few μm to tens of nm resolution in three dimensions.

Tomography experiments generate a large amount of data in a relatively short time and demands much computing power for image processing and reconstruction calculations. A high speed data transfer network and a high performance computer system are therefore needed to complement the high data acqusition rate to give facility users a prompt feedback of the reconstruction results. This is particularly valuable for user-shared facilities where each user has only a limited days of operation annually. A quasi-realtime x-ray tomography system has been constructed at the 2BM (bending magnet) beamline at the Advanced Photon Source (APS) at Argonne National Laboratory. It uses a scintillated CCD based direct projection imaging system to acquire x-ray projections and trasfers the projections to a parallel computer located at the Mathematics and Computer Science Division (MCS) for the preprocessing and reconstruction calculations. Using this remote computing scheme, the computation time is approximately equal to

the acquisition time so that the reconstruction result from the data acquired at experimental station can be viewed by the operators shortly after the data is acquired.

2. DATA ACQUISITION SYSTEM

The 2BM beamline was constructed originally for deep x-ray lithography exposure by Lai, *et. al.*[7] and later x-ray microtomography experiments was developed for the beamline by Lee, *et. al.*.[3] A direct projection system shown in Fig. 1 is used to acquire the tomogrpahic projections. The x-ray beam emitted from the bending magnet is monochromatized by a Kohzu double crystal monochromator then apertured to a 5×5 mm^2 size. The sample is placed in the apertured beam and the transmitted x ray illuminates a $CdWO_4$ single crystal scintillator. The visible light emitted by the scintillator is imaged to a CCD detector by a visible light microscope objective. A 10× objective with numeric aperture of 0.2 is frequently used, but in the current setup, its effective magnification is approximately 5× and its numeric aperture is about 0.1. The scincillator screen is effectively grainless and resolution of the system is determined primarily by the combination of the resolution of the objective and the CCD pixel size. Using the Rayleigh criterion, the resolution of the objective can be estimated to be

$$\delta = 0.61 \times \frac{\lambda}{\text{N.A.}} \approx 0.61 \times \frac{0.5}{0.1} \approx 3\ \mu\text{m}. \tag{1}$$

On the other hand, the CCD has pixel size of 6.8 μm, correspoonding to roughly 1.4 μm pixel size at the sample plane. Therefore we estimate the resolution of the images to be about 3 μm, or 2 pixels. This setup approximately satisfies the Nyquist sampling theorem. The resolution can be imporved to higher than 1 μm by using a different objective at the cost of small field of view.[3]

Using this system, the sample's complex index of refraction along with the distance between the sample and scintillation screen determined whether phase or absorption is the predominant contrast mechanism of the recorded images. Fig. 2 shows one projection of a micromachined gear acquired in phase contrast during a live demonstrations of this system at the 1998 SuperComputing Conference and Fig. 3 shows one projection of an ant's head acquired in absorption contrast mode during a recent test.

For each projection, typically 1024×1024 images are acquired in 10 seconds integration time, or 512×512 images can be acquired in 3 second integration time with 2×2 binning. The CCD data transfer time is about 3 seconds for 1024×1024 size images and 1 second for 512×512 size images. After each image is acquired, it is saved on a local hard drive, and immediately after the data file is saved, a ftp daemon transfers it to the SGI parallel computer at MCS. A tomographic data set is usually acquired in a few cycles, starting with coarse then finer angular spacings. The reconstruction from the coarse angluar steps is usually completed well before the the acquisition of the fine angular finishes. Therefore the user can view the reconstruction results from the coarsely spaced data when the projections of finer angular spacings are being acquired. This gives the user an opportunity to change parameters for preprocessing, reconstruction, and visualization, or to abort the acquisition. The acquisition sequence is currently controled by a script written in IDL (Interactive Data Language, Research Systems, Inc.) and a graphical user interface is currently being developed.

3. COMPUTING STRUCTURE

The data files transfered from the data acquistion system to the parallel computer stores information on experimental facility, beamline, and data acquisition system. It also contains information on the image processing routines to be applied to the projections and the reconstruction methods to be used along with the parameters for each operation. After the data files arrive at the parallel computer, they undergo several prelimary image processing steps such as normalization and alignment. The projections are then assembled into sinograms and reconstructed into volume slices. The reconstrution volume are then directed into another parallel computer to generate rendered images for viewing at video rate at both the MCS Division and the experimental floor. Rendered still images are also written periodically to a web server to be viewed by collaborators world wide. This pipelined data acquisition and computation system is illustrated in Fig. 4.

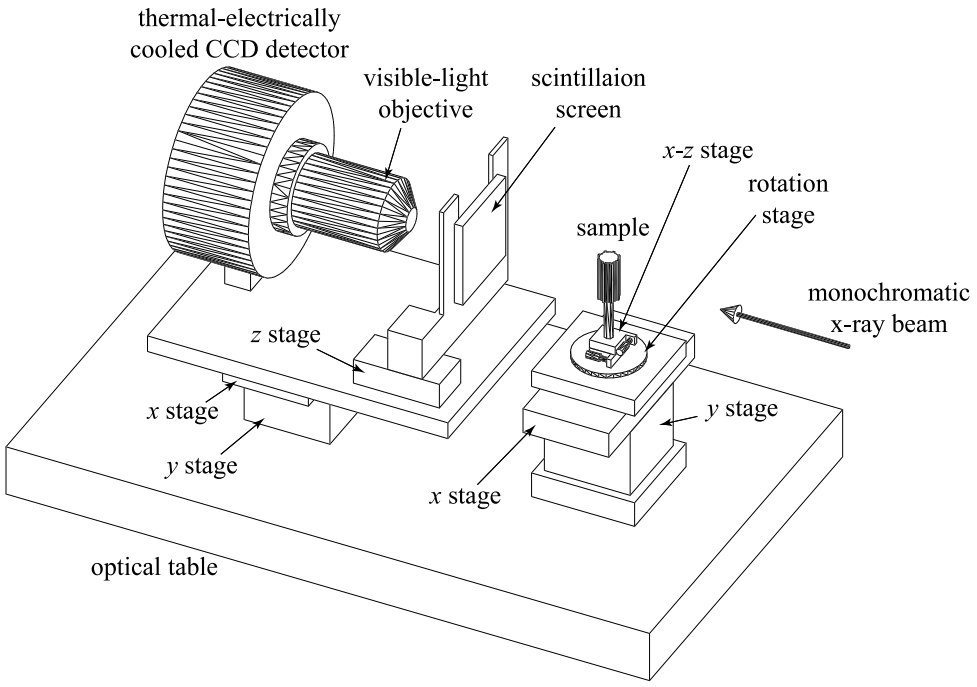

Figure 1. The straight-ray projection imaging scheme used to acquire the tomographic projections. The x-ray beam is monochromatized by a Kohzu double crystal grating. The monochromatic beam passes through the sample and reaches the $CdWO_4$ single crystal scintilation screen. The visible light emitted by the scintillator is relayed to the CCD detector by a microscope objective. Both the sample and the detector are mounted on x-y stages for alignment to the x-ray beam. The sample is fixed on a minature x-z stage mounted on the rotation stage so that the sample's region of interest can be centered on the rotation axis. The scintillation screen is mounted on a z stage for visible-light objective focusing adjustment.

3.1. Data File Structure

The data from the acquisition system are separated into a header file containing the experimental conditions and a series of data files that contain the actual projection data. The structure of the hdf header file is shown in Fig. 5. The files are written in the Hierachical Data Format (HDF) created by the National Center for Supercomputing Applications.[8] The hdf format was chosen because of the following benefits:

- It is platform independent.
- It is self-describing.
- It supports nearly all data types that are likely to be used in experiments.
- It has a hierachical structure to organize a large number of data fields.

The content of the files are organized on the basis of NeXus convention developed at Argonne National Laboratory for the exchange of data from neutron and synchrotron source based experiments.[9,10] The original NeXus data group definitions have been extended to accommodate the additional information required for tomography applications. An API written in C++ was implemented to manage the data. The API has C++ class definitions that correspond to the hdf data structures.

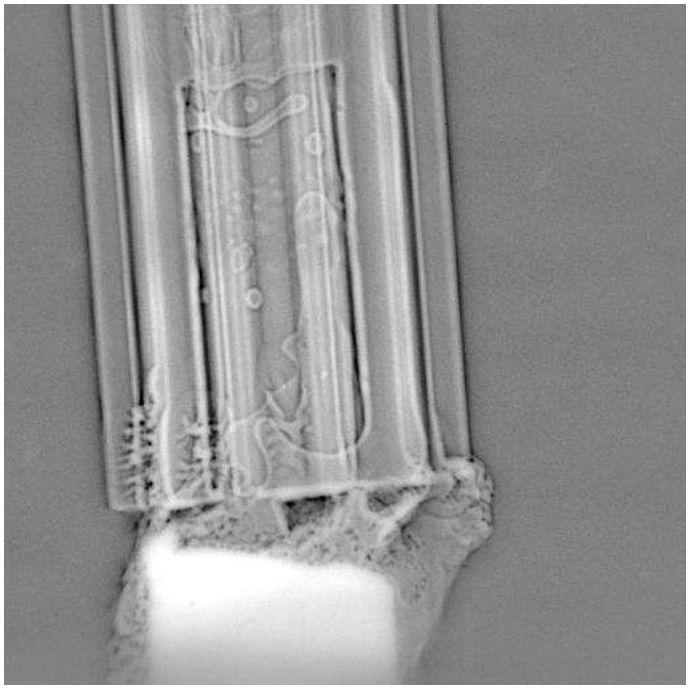

Figure 2. One projection of a micromachined gear acquired using 15 KeV x ray using phase contrast. The gear was fabricated at 2BM beamline with deep x-ray lithgraphy technique. It was made of PMMA with gold coating. The diameter of the gear is about 100 μm and the image consists of 512×512 pixels.

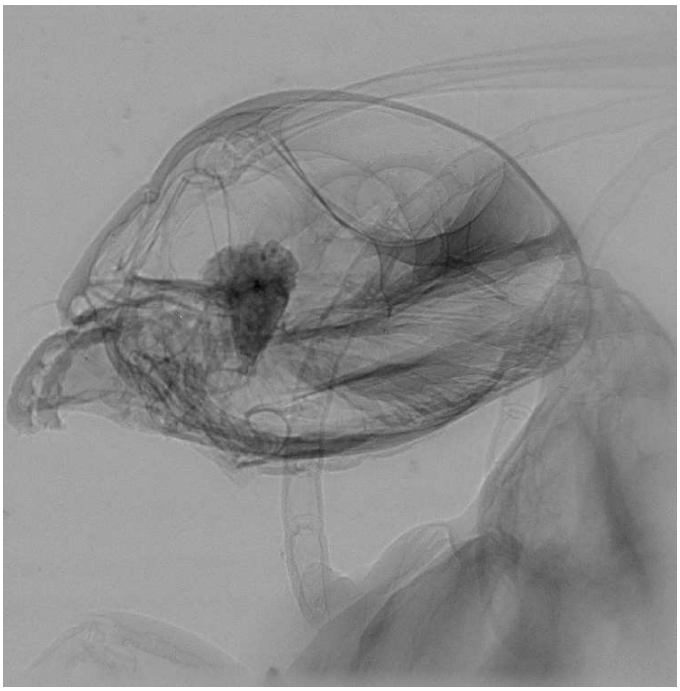

Figure 3. One projection of a carpenter ant's head acquired using 9 KeV x ray in absorption contrast mode. The field size was about 1.5 mm with 1024×1024 pixels.

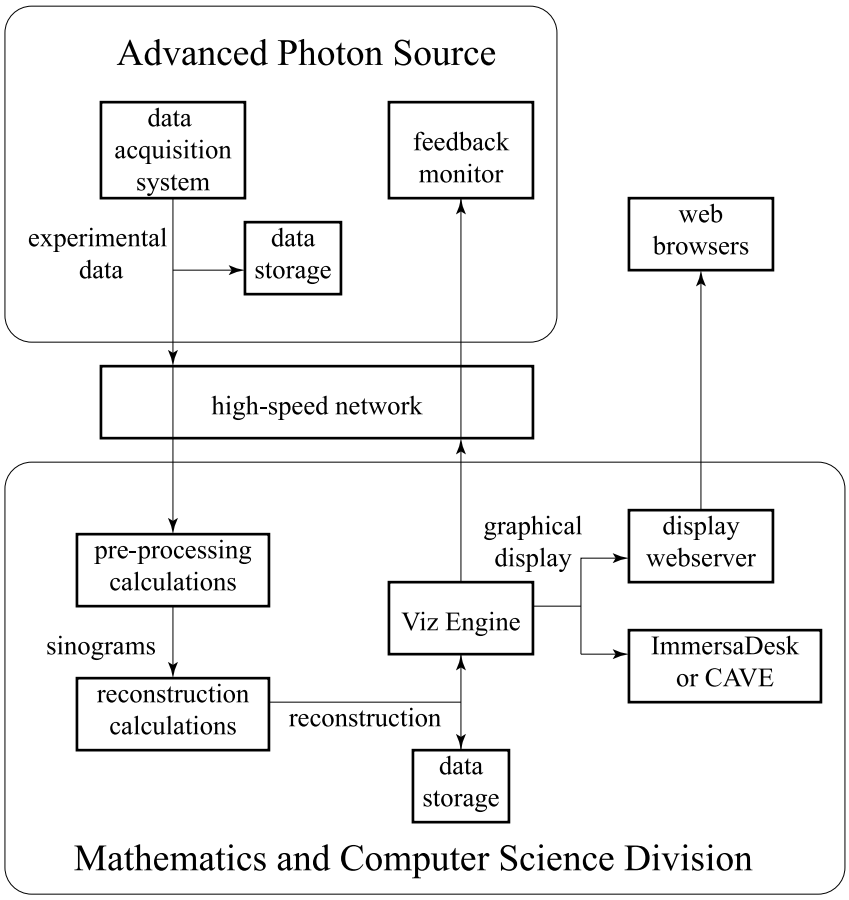

Figure 4. Illustration of the data acquisition and computation pipeline. An operator at the experimental station in the Advanced Photon Source controls the data acquisitoin system and views the reconstruction result on the feedback monitor. The data acquired at the beamline is first written to a local hard disk and then transfered via a 100 Mb/second network to the Mathematics and Computer Science Division. The preprocessing and reconstruction calculations are performed by the parallel computer. The reconstruction results are saved to a hard disk at MCS then fed into the Viz Engine. The Viz Engine provides volume rendering images interatively to the beamline feedback monitor via the high-speed network and also periodically writes rendered still images to a web server.

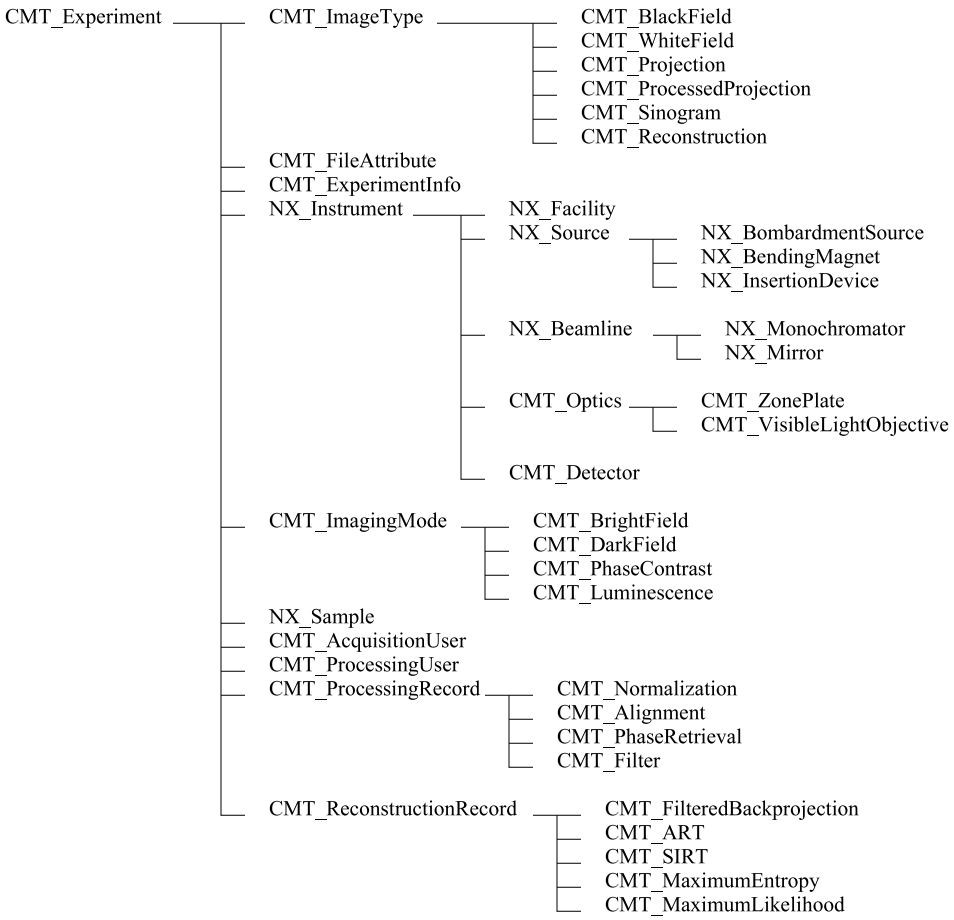

Figure 5. Group structure of the hdf header file and the classes structure of the API written in C++. A time stamp and file version are stored in the CMT_FileAttribute. Information on the experiment operator and the experiment are stored in CMT_AcquisitionUser and CMT_ExperimentInfo groups. Experimental conditions, such as the facility, beamline, optics, detectors, and sample information are stored in NX_Instrument and NX_Sample. The imaging mode or contrast mechanism is stored in CMT_ImagingMode. Only one imaging mode is used for each header file. The header file also contains information on the type of images stored in the series of associated data files: for example, CMT_WhiteField and CMT_Projections are present in the raw data files while CMT_Sinogram is present in a series of files containing sinograms. The groups CMT_ProcessingUser, CMT_ProcessingRecord, CMT_ReconstructionRecord store information on the person performing the image processing and reconstruction along with the processing procedure and reconstruction methods used.

3.2. Parallel Computer System

A SGI Origin 2000 parallel computer with 128 nodes is used for the computations. It utilizes a grid-enabled computing environment with the Globus metacomputing toolkit.[11] Analogous to eletric power grids, the Globus framework dynamically handles resource allocation, resource configuration, program submission, I/O operation, program scheduling, file staging, and uniform program executions within a system of processors or work stations.[12]

After the reconstructions are completed, the results are transfered to another SGI workstation call the Viz Engine for visualization calculations. The visualization software running on the Viz Engine software uses a hardware-optimized volume rendering fuction library from Silicon Graphics called the Volumizer.[13] The rendered images can be viewed as a stereoscopic display on an ImmersaDesk in realtime at live video frame rate as the data volume is manipulated or as displayed parameters are changed. One limitation is that the data volume must have a size less than $256 \times 256 \times 256$ pixels, hence our reconstructions often need to be subsampled before they can be loaded into the Viz Engine. The Viz Engine also periodically writes still images of the volume rendering to a web server so that the rendered displays can be viewed by collaborators worldwide. This feature is especially useful for experiments with wide range of participation since besides reducing the travel cost for the collaborators it also allows a large number of specialist to provide prompt interpretation and feedback to the experiment operators.

3.3. Image Processing and Reconstruction

A number of image processing operations are applied to the projection data before they are assembled into sinograms for reconstruction. An increasing collection of filters are being added to this preprocessing software package and they can be selectively invoked by the user. The following are the currently implemented routines:

- *white field removal*: Removes the white field background of an image according to the Lambert-Beer law of x-ray absorption:
$$f' = \ln \frac{f_0}{f}, \tag{2}$$
where f is the raw image, f_0 is the white field image and f' is the filtered image.
- *mean and median filter*: Replaces a pixel by a local average or median.
- *zinger filter*: Calculates the local mean (or median) and standard deviation at each image pixel. Replace the pixel by the mean (or median) if the pixel value is more than a certain standard deviations away from the mean (or median).
- *Wiener fitler (least square)*: Deconvolution using a predetermined point spread function weighed by the signal-to-noise spectrum.

The white field removal function is routinely used in the experiments to remove artifacts resulted from imperfections of the scintillation screen and beam non-uniformity. The mean/median and zinger filters are sometime invoked to remove noisey pixels from images. After the projections are filtered, they must be aligned so that they appear to rotate around a common axis. Two alignment algorithms are currently implemented:

- *centroid matching*: Shifts an image so that its centroid is located at a predetermined position.
- *cross-correlation*: Aligns two images to each other using the cross-correlation function.

Alignment using the cross-correlation method is more accurate and consistent but more time consuming and difficult to parallelize. For this reason, the centroid matching method is often used in the live run while the cross-correlation method is mostly used in post-processing mode.

The reconstruction routines "ptomo" are based on code provided by Mark Ellisman and Steve Young from the National Center for Microscopy and Imaging Research at the San Diego Supercomputing Center.[14] Three algorithms are implemented: filtered backprojection, ART and SIRT. Because of the large number of projections acquired in our experiments, filtered backprojection has been used in our demostrations and tests. Figures 6 and 7 show the screen captures from the visualization computer displaying the gear and ant data. They are of lower resolution than the reconstruction because of subsampling. A section of the ant's head reconstruction without the subsampling is

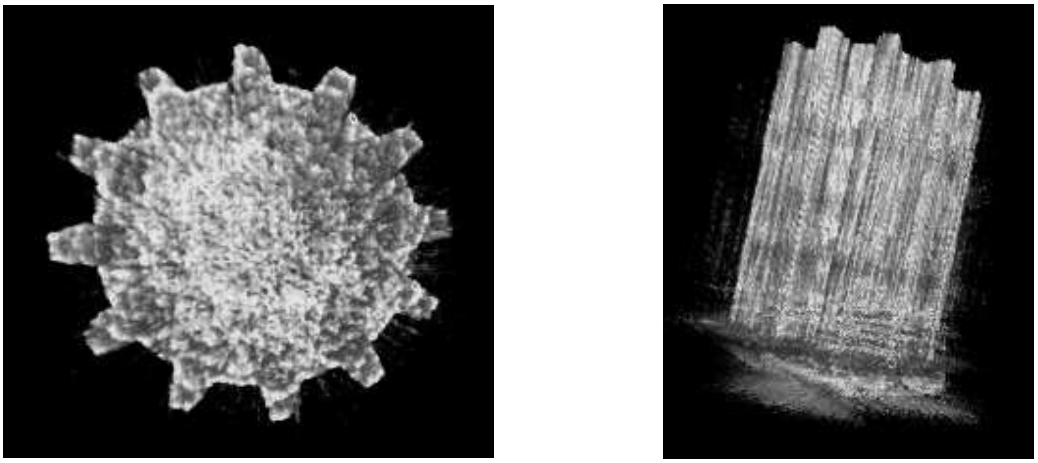

Figure 6. Reconstruction from the micromachined gear data. A section perpendicular to the gear axis is shown on the left and a side view is shown on the right. (Screen captures, subsampled to 256×256×256.)

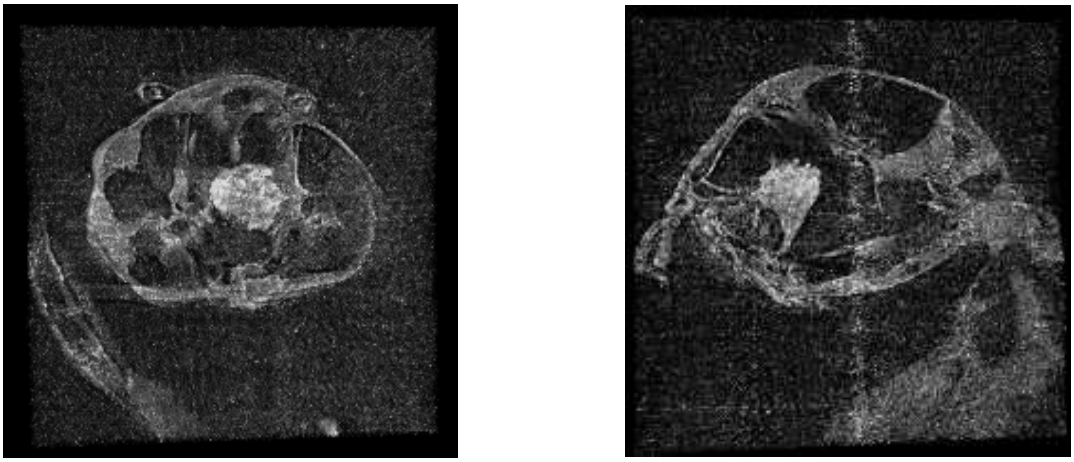

Figure 7. Sections of the reconstruction from the ant data. A "horizontal" section is shown at the left and a "vertical" section is shown at the right. (Screen captures, subsampled to 256×256×256.)

shown in Fig. 8. From our demo and test runs with 180 projections each consisting of 512×512 16 bit integers, and using 20 of the 128 processors, the preprocessing and reconstruction calculations can be completed in less than 10 minutes. When the data were acquired in a few cycles, the reconstruction from the starting cycles of typically only 12 to 24 projection can be viewed at the experimental station with 2 to 3 minutes.

4. DISCUSSION

This hard x-ray microtomography systems has demontrated quasi-realtime acquisition and reconstruction in tens of minutes scale. Currently the processes of data acquistion and computation take about same amount of time, thus the two steps are "synchronized." We would like to reduce both time intervals so that the time requirment for the pipeline is only limited by the photon flux of the synchrotron. A number of changes have been planned to decrease the acquisition time to a few seconds:

- The beamline efficiency can be improved dramatically by using multilayer mirrors and a grating monochromator.

Figure 8. One section from the reconstruction using the ant data. The images consists of 512×512 pixels of 3 μm size.

- The sicintillated detection system needs a scintillator better matched for 5-20 KeV energies range and a high numerical aperture objective.

These two improvments can increase the combined efficiency of the beamline and the detection system by a factor of 10^4. Therefore the acquisition times can be reduced to 1 second scale if the CCD readout time can be improved correspondingly. On the other hand, the computation time can also be reduced to under 1 minute for 180 projections of 512×512-pixel images with the following improvments:

- The preprocessing routines will be streamlined and parallelized.
- The reconstruction software ported from the San Diego Supercomputing Center will be optimized for our computing platform acquisition scheme.

We are also planning to improve the spatial resolution of our tomography system on two fronts: a better scintillation screen and high numerical aperture objective can increase the resolution of our current setup to 1 μm, or alternatively a PEEM based detection system has the potential of increasing the resolution to 10 nm scale; an imaging type microscope is being developed at 2ID-B (insertion device) beamline at APS using 1-4 KeV soft x rays and a zone plate optical element for magnification to produce 50 nm resolution. We are also making an effort to develop a graphical user interface system to control the acquisition, preprocessing, reconstruction, visualization steps so that this system can be used by general beamline users.

ACKNOWLEDGMENTS

This work is supported by the U.S. Department of Energy, Office of Basic Energy Sciences, Division of Material Sciences, under contract W-31-109-ENG-38.

REFERENCES

1. T. M. Breunig, J. C. Elliot, S. R. Stock, P. Anderson, G. R. Davis, and A. Guvenilir, "Quantitative characterization of damage in a composite material using x-ray tomographic microscopy," in *X-ray Microscopy III*, A. G. Michett and G. R. Morrison, eds., pp. 465–468, Springer-Verlag, Berlin, 1991.
2. J. H. Kinney, M. C. Nichols, U. Bonse, S. R. Stock, T. M. Breunig, A. Guvenilir, and R. A. Saroyan, "Nondestructive imaging of materials microstructures using x-ray tomographic microscopy," in *Materials Research Society Sym. Proc.*, Ackerman and W. A. Ellingson, eds., pp. 85–95, Materials Research Society, Pittsburg, 1990.
3. H.-R. Lee, B. Lai, W. Yun, D. C. Mancini, and Z. Cai, "X-ray microtomography as a fast three-dimensional imagin technology using a ccd camera coupled with a $cdwo_4$ single-crystal scintillator," in *SPIE Proc.*, vol. 3149, p. 257, Society of Photo-Optical Instrumentation Engineers (SPIE), (Bellingham, Washington), 1997.
4. W. S. Haddad, I. McNulty, J. E. Trebes, E. H. Anderson, R. A. Levesque, and L. Yang, "Ultra high resolution x-ray tomography," *Science* **266**, pp. 1213–1215, 1994.
5. J. Lehr, "3D x-ray microscopy: tomographic imaging of mineral sheaths of bacteria *Leptothrix ochracea* with the Göttingen x-ray microscope at BESSY," *Optik* **104**(4), pp. 166–170, 1997.
6. Y. Wang, C. Jacobsen, J. Maser, and A. Osanna, "Soft x-ray microscopy with a cryo stmx: Tomography," *Journal of Microscopy* , p. in press, 1999.
7. B. Lai, D. C. Mancini, W. Yun, and E. Gluskin, "Beamline and exposure station for deep x-ray lithography at the advanced photon source," in *SPIE Proc.*, vol. 2880, p. 171, Society of Photo-Optical Instrumentation Engineers (SPIE), (Bellingham, Washington), 1996.
8. *NCSA hdf homepage:* `http://hdf.ncsa.uiuc.edu/`.
9. P. Klosowski, M. Koennecke, J. Z. Tischler, and R. Osborn, "Nexus: A common format for the exchange of neutron and synchrotron data," *Physica* .
10. *NeXus homepage:* `http://www.neutron.anl.gov/NeXus`.
11. I. Foster and C. Kesselman, *The Grid: Blueprint for a New Computing Infrastructure*, Morgan Kaufman, 1998.
12. G. von Laszewski, J. A. Insley, I. Foster, J. Bresnahan, C. Kesselman, M.-H. Su, M. Thiebaux, M. L. Rivers, S. Wang, B. Tieman, and I. McNulty, "Real-time analysis, visualization and steering of microtomography experiment at photon sources," in *SuperComputing, Proc.*, vol. 217, p. 314, Publisher, (Address), 1998.
13. R. Drebin, L. Carpenter, and P. Hanrahan, "Volume rendering," in *Proceedings of SIGGRAPH'88*, pp. 65–74, August, 1988.
14. P. J. Mercurio, T. T. Elvins, S. J. Young, P. S. Cohen, K. R. Fall, and M. H. Ellisman, "The distributed laboratory: An interative visualization environment for electron microscopy and three-dimensional imaging," *Comm. Assoc. Comp. Mach.* .